

# Predictive value of CT imaging findings in COVID-19 pneumonia at the time of first-screen regarding the need for hospitalization or intensive care unit

Deniz Esin Tekcan Sanli 

Duzgun Yildirim 

Ahmet Necati Sanli 

Neval Erozan 

Guray Husmen 

Aytug Altundag 

Filiz Tuzuner 

Oner Dikensoy 

Ceyda Erel Kirisoglu 

## PURPOSE

In this study, we aimed to reveal the relationship between initial lung parenchymal involvement patterns and the subsequent need for hospitalization and/or intensive care unit admission in coronavirus disease 2019 (COVID-19) positive cases.

## METHODS


Overall, 231 patients diagnosed with COVID-19 as proven by PCR were included in this study. Based on the duration of hospitalization, patients were divided into three groups as follows: Group 1, patients receiving outpatient treatment or requiring hospitalization <7 days; Group 2, requiring hospitalization ≥7 days; Group 3, patients requiring at least 1 day of intensive care at any time. Chest CT findings at first admission were evaluated for the following features: typical/atypical involvement of the disease, infiltration patterns (ground-glass opacities, crazy-paving pattern, consolidation), distribution and the largest diameters of the lesions, total lesion numbers, number of affected lung lobes, and affected total lung parenchyma percentages. The variability of all these findings according to the groups was analyzed statistically.

## RESULTS

In this study, 172 patients were in Group 1, 39 patients in Group 2, and 20 patients in Group 3. The findings obtained in this study indicated that there was no statistically significant difference in ground-glass opacity rates among the groups ( $p = 0.344$ ). The rates of crazy-paving and consolidation patterns were significantly higher in Groups 2 and 3 than in Group 1 ( $p = 0.001$ ,  $p = 0.002$ , respectively). The rate of right upper, left upper lobe, and right middle lobe involvements as consolidation pattern was significantly higher in Group 3 than in Group 1 ( $p = 0.148$ ,  $p = 0.935$ ,  $p = 0.143$ , respectively). A statistically significant difference was also found between the affected lobe numbers, total lesion numbers, the diameter of the largest lesion, and the affected lung parenchyma percentages between the groups ( $p = 0.001$ ). The average number of impacted lobes in Group 1 was 2; 4 in Group 2 and Group 3. The mean percentage of affected lung parenchyma percentage was 25% in Group 1 and Group 2, and 50% in Group 3.

## CONCLUSION

In case of infiltration dominated by right middle or upper lobe involvement with a consolidation pattern, there is a higher risk of future intensive care need. Also, the need for intensive care increases as the number of affected lobes and percentage of affected parenchymal involvement increase.

From the Departments of Radiology (D.E.T.S.  [tekcandenizesin@gmail.com](mailto:tekcandenizesin@gmail.com), N.E., G.H.) and Pulmonary Medicine (C.E.K), Acibadem Kozyatagi Hospital, Istanbul, Turkey; Departments of Radiology (D.Y.), Otolaryngology (A.A.), Anesthesiology (F.T.), and Pulmonary Medicine (O.D.), Acibadem Taksim Hospital, Istanbul, Turkey; Department of General Surgery (A.N.S.), Istanbul University-Cerrahpasa, Cerrahpasa Medical Faculty, Istanbul, Turkey.

Received 4 June 2020; revision requested 30 June 2020; last revision received 11 September 2020; accepted 15 September 2020.

Published online 2 December 2020.

DOI 10.5152/dir.2020.20421

Coronavirus disease 2019 (COVID-19), initially reported in China in late 2019, has caused a rapidly spreading worldwide pandemic. It is a serious disease that arises from acute respiratory syndrome coronavirus-2 (SARS-CoV-2), which mainly affects the respiratory tract (1). The gold standard method in diagnosis is the reverse transcriptase-polymerase chain reaction (RT-PCR) test, which is studied from nasopharyngeal and/or oropharyngeal swab specimens. Although its specificity is high, its sensitivity varies according to the sensitivity of the kit, the method of sampling, and the person taking the sample (30%–85%) (2, 3). Also, it takes a few days to get the results of the test. Chest CT has been widely used for diagnostic purposes despite the radiation limitation since it is possible to detect typical infiltration pattern of the disease even in the absence of obvious clinical symptoms in the hyperacute period at initial admission to the hospital (4).

You may cite this article as: Tekcan Sanli DE, Yildirim D, Sanli AN, et al. Predictive value of CT imaging findings in COVID-19 pneumonia at the time of first-screen regarding the need for hospitalization or intensive care unit. *Diagn Interv Radiol* 2021; 27: 599–606

Clinical experience and studies up to date indicate that the disease progresses more rapidly with poor clinical outcomes when presented in elderly patients (>65 years), males, and those with comorbidities (5). Some laboratory parameters such as C-reactive protein (CRP), D-dimer, neutrophil lymphocyte ratio (NLR) are increased in this group, which carry a higher risk in terms of complications, including multiorgan failure, sepsis, and mortality (6, 7).

Our aim in this study was to evaluate the prognostic value of chest CT findings at initial admission and its predictive value for subsequent hospitalization or intensive care unit (ICU) admission. Additionally, we assessed the importance of involvement patterns and the extent of infiltration for this prediction. Our ultimate aim was to describe findings that facilitate the triage of the patients and stratify patients before the clinical course deteriorates.

## Methods

### Study population

Ethical approval was obtained for this retrospective study (2020-05/28), and informed consent forms were obtained before CT acquisition. In this retrospective study, 1300 patients who were admitted to our hospital with symptoms of cough, fever, myalgia, smell-taste disorders, or flu-like upper respiratory tract infection with a suspected diagnosis of COVID-19 between 11 March and 11 April were evaluated. At initial admission, all cases were examined by emergency, pulmonary medicine and/or infectious disease physicians, and were evaluated for comorbidities (diabetes, hypertension, asthma, chronic obstructive pulmonary disease [COPD]), smoking habit, laboratory findings (CRP, lymphocyte count, NLR, ferritin, lactate dehydrogenase [LDH], D-dimer and procalcitonin), symptomatology (fever, cough, shortness of breath, respiratory distress ( $\text{PaO}_2 < 93\%$  or respira-

tory rate >20), and PA chest X-ray/chest CT findings. Cases with a runny nose, sneezing, eye redness/itching, and those with a dry cough and sneezing were excluded from the study. Chest CT was performed on 890 patients. A total of 231 patients diagnosed with PCR-proven COVID-19 and who started medical treatment were included in this study. According to the course of hospitalization, patients were allocated into three groups as follows: Group 1, patients appropriate for outpatient treatment or requiring hospitalization less than 7 days; Group 2, patients requiring hospitalization more than 7 days; Group 3, patients requiring at least 1 day in the ICU at any time (Fig. 1).

### Imaging procedure

All CT scans were done with Siemens Somatom Sensation-Syngo CT 2009 device using a low-dose noncontrast CT protocol. Patients were scanned in the supine position during deep inspiration. The acquisition parameters were standardized as: tube voltage, 140 kV; tube current, 40 mA; pitch, 1.4; FOV, 455 mm; slice thickness, 64×0.6

mm. Images were converted into 1 mm thin reconstructions in the lung parenchyma window. The 8 mm MIP images were also created in coronal, sagittal, and axial plans by postprocessing procedures and sent to the PACS archiving system. The rules of isolation and disinfection were followed during and after the scanning. Mask and other personal protective equipment were mandatory for technicians, patients, and cleaning staff. The interval between consecutive patients was at least 15 minutes.

### Image analysis

All images were evaluated separately by two radiologists with approximately 20 years (D.Y.) and 10 years (N.E.) of practical experience in chest CT in the hospitals. Radiologically typical/atypical presentations of cases were evaluated according to the criteria of the Radiological Society of North America (RSNA) Expert Consensus Statement on Reporting Chest CT Findings Related to COVID-19, as of April 2020 (18). Specific CT findings (GGOs, crazy-paving pattern, consolidation, vascular enlarge-

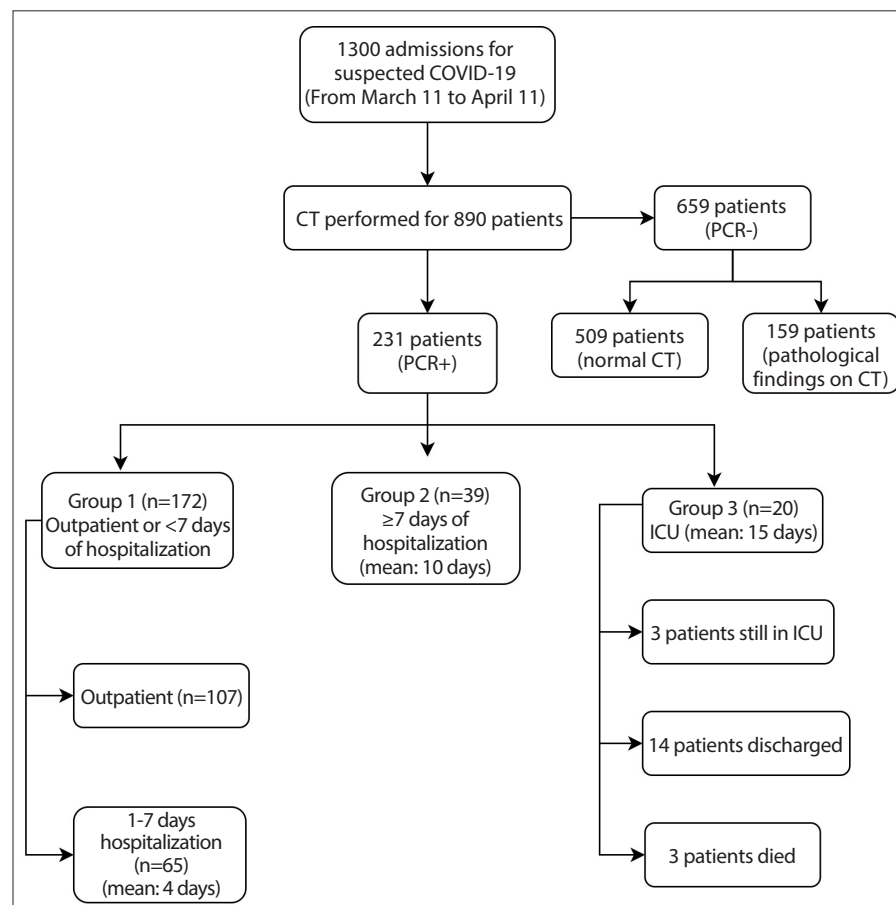


Figure 1. Diagram shows the total number of patients and the mean duration of hospitalization by groups.

### Main points

- Chest CT imaging findings for COVID-19 pneumonia depend on multiple factors.
- Estimating the prognosis of COVID-19 pneumonia with only CT imaging features may be misleading.
- The need for hospitalization increases if there is extensive infiltration in the form of consolidation.

ment, halo sign, reverse halo sign, fibrotic band, vacuolar sign) and atypical imaging findings (tree-in-bud, lobar consolidation, mediastinal lymphadenopathy (LAP) (>1 cm), pleural thickening, pleural effusion) of the disease were documented. The distribution of GGOs, crazy-paving, and consolidation patterns were classified as peripheral (distal 1/3 of lung parenchyma), central and diffuse. The total number of lesions, the diameter of the largest lesion, and the percentage of affected total lung parenchyma (1, <25%; 2, 25%–50%; 3, 50%–75%; 4, >75%) were also calculated in multiplanar images. The affected lung areas were measured electronically in continuous reconstructed axial sections 10 mm section thickness, then the sum of the sequential areas was recorded. These measurements were all achieved by MPR images with Syngo.Via Software (VB10B, Siemens). In atypical or suspicious cases, CT images were reevaluated together and a consensus was reached. Interobserver reliability was calculated.

The effects of smoking and comorbid diseases (diabetes, hypertension, asthma, COPD, others) on hospitalization needs were statistically examined. At the same time, the relationship between clinical symptoms of patients (fever [ $> 37^{\circ}\text{C}$ ], shortness of breath [ $\text{PaO}_2 < 93\%$  or respiratory rate  $> 20$ ], dry cough), laboratory findings specific to the disease (lymphocyte count, NLR, CRP, D-dimer, ferritin, LDH, procalcitonin) and the duration of hospitalization were evaluated. Also, the interval between the symptom onset and admission to the hospital was evaluated for each group.

### Statistical analysis

NCSS (Number Cruncher Statistical System) 2007 program was employed to analyze the data. To evaluate the data obtained in this study, numerical variables were presented as median (minimum-maximum) for non-normally distributed variables, mean and standard deviation for the normally distributed variables. Categorical variables were reported as frequencies and percentages. One-way ANOVA test was used for three or more group comparisons of variables that meet normality conditions, and Bonferroni test was used for binary comparisons. Kruskal Wallis test was used for comparison of three or more groups, Bonferroni-Dunn test was used for paired comparisons of variables that did not meet normality requirements. Pearson chi-square

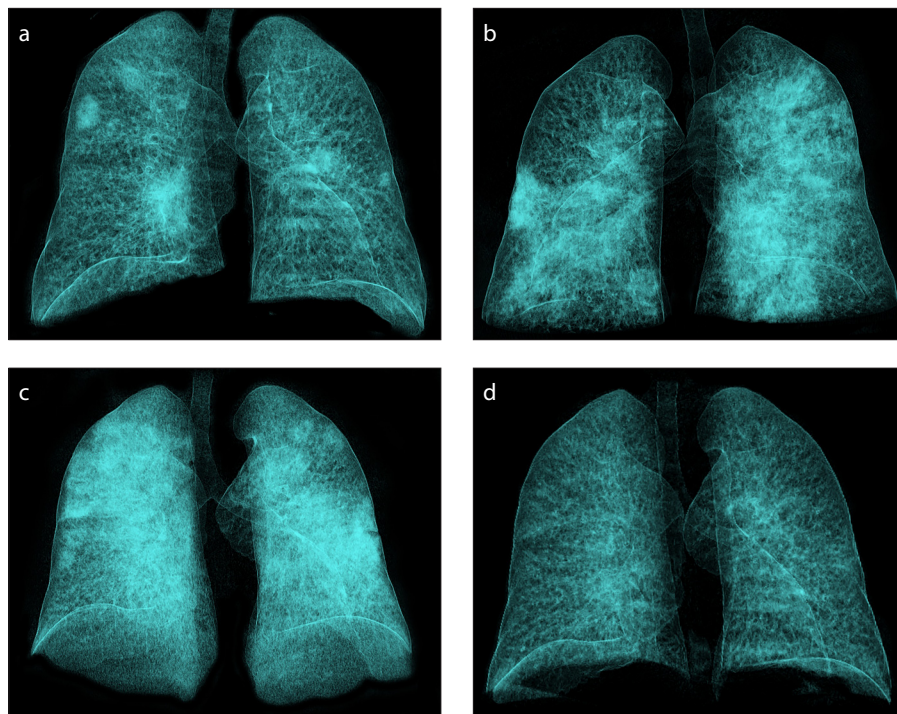


**Figure 2. a–d.** Demonstration of the normal evolution of the disease during a one-month course in a 46-year-old immunocompetent patient by volume-rendered 3D reconstruction in CT images (RadiAnt DICOM Viewer 5.5.1; Medixant). Chest CT image (a) at initial acquisition shows peripheral and central lesions affecting both lower and upper lobes. Control CT image (b) 5 days later shows diffuse infiltration affecting all lobes, especially on the left. CT image (c) 13 days after admission shows bilateral diffuse lung involvement with sparing of apical segments (white lung). CT image (d) at one-month follow-up shows interval marked regression of parenchymal findings.

was used when comparing categorical variables, further analyses were made with  $2 \times 2$  contingency table to test whether a significant difference is present among groups. In  $R \times C$  tables with more than 20% of expected counts less than 5, Fisher-Freeman-Halton Exact test was used. The conformity of the quantitative data given normality was tested by Kolmogorov-Smirnov, Shapiro-Wilk test and graphical evaluations.  $p < 0.05$  was accepted as statistically significant. Interobserver agreement between the two readers for radiological parameters was calculated by the  $\kappa$  coefficients.

## Results

Overall, 172 patients (74%) were in Group 1, 39 patients (17%) in Group 2, and 20 patients (9%) in Group 3. Patient age ranged between 5 and 94 years, with a mean of  $48.1 \pm 15.6$  years (Table 1). Mean age of Group 1 patients was significantly lower compared to Groups 2 and 3 ( $p = 0.004$ ;  $p = 0.001$ , respectively). Sex of the patients was not significantly different between groups ( $p = 0.555$ ). Comorbid diseases were detected increasingly according to the groups. Diabetes, hyperten-

sion, COPD was significantly more prevalent in Group 3 ( $p = 0.001$ ,  $p = 0.001$ ,  $p = 0.004$ , respectively). No significant difference was found between asthma and smoking history among the groups ( $p = 0.740$ ,  $p = 0.143$ ). Fever, cough, and shortness of breath at initial admission were significantly more frequent in Groups 2 and 3 than Group 1 ( $p = 0.001$ ,  $p = 0.030$ ,  $p = 0.001$ , respectively). Lymphocyte counts, NLR, CRP, and D-dimer values varied according to the groups and were found to be significantly higher in Group 3 ( $p = 0.001$ ,  $p = 0.002$ ,  $p = 0.001$ ,  $p = 0.008$ , respectively). The demographic features, symptomatology, comorbid diseases, laboratory findings of the patients' are detailed in Table 1. The interval between symptom onset and admission to the hospital was  $4.7 \pm 1.8$  days (1–8 days) in all patients,  $5 \pm 1.7$  days (1–8 days) in Group 1,  $5 \pm 2$  days (2–8 days) in Group 2, and  $3.1 \pm 1.8$  days (1–7 days) in Group 3. Fig. 2 shows normal evolution of the disease during a 1-month course in a hospitalized immunocompetent patient by volume-rendered 3D reconstruction CT images.

Fourteen patients had no ground-glass opacity (GGO) on CT examination. Of these,

**Table 1.** Demographic features, symptoms, comorbid diseases, and laboratory findings by groups

		Groups			<i>p</i>	Post hoc test
		Outpatient (n=172)	Inpatient (n=39)	ICU (n=20)		
Age	Mean ± SD	45.0±14.4	53.2±14.6	65.0±14.2	<0.001 <sup>a</sup>	1-2, <i>p</i> = 0.004; 1-3, <i>p</i> < 0.001; 2-3, <i>p</i> = 0.010
Sex, n (%)	Male (n=147)	106 (61.6)	27 (69.2)	14 (70.0)	0.555 <sup>b</sup>	NS
	Female (n=84)	66 (38.4)	12 (30.8)	6 (30.0)		
Comorbidity, n (%)	Diabetes mellitus (n=42)	20 (11.62)	12 (30.76)	10 (50.0)	<0.001 <sup>b</sup>	1-2, <i>p</i> = 0.003; 1-3, <i>p</i> < 0.001;
	Hypertension (n=63)	31 (18.02)	18 (46.15)	14 (70.0)	<0.001 <sup>b</sup>	1-2, <i>p</i> < 0.001; 1-3, <i>p</i> < 0.001;
	Asthma (n=17)	14 (8.13)	2 (5.12)	1 (5.0)	0.740 <sup>b</sup>	NS
	COPD (n=28)	14 (8.13)	8 (20.51)	6 (30.0)	0.004 <sup>b</sup>	1-3, <i>p</i> = 0.009
	Others (n=25)	13 (7.55)	4 (10.25)	8 (40.0)	<0.001 <sup>b</sup>	1-2, <i>p</i> = 0.038; 1-3, <i>p</i> < 0.001; 2-3, <i>p</i> = 0.014
	Smoking habitus (n=40)	26 (15.11)	11 (28.20)	3 (15.0)	0.143 <sup>b</sup>	NS
Fever (n=120), n (%)		74 (43.02)	29 (74.35)	17 (85.0)	<0.001 <sup>b</sup>	1-2, <i>p</i> < 0.001; 1-3, <i>p</i> < 0.001;
Shortness of breath (n=48), n (%)						
(PaO <sub>2</sub> <93% or respiratory rate > 20)		6 (3.48)	24 (61.53)	18 (90.0)	<0.001 <sup>b</sup>	1-2, <i>p</i> < 0.001; 1-3, <i>p</i> < 0.001; 2-3, <i>p</i> = 0.022
Cough (n=162)		113 (65.69)	31 (79.48)	18 (90.0)	0.030 <sup>b</sup>	1-3, <i>p</i> = 0.027;
Lymphopenia (<13×10 <sup>3</sup> /uL) (n=183)		(n=125)	(n=38)	(n=20)		
	Low	41 (32.8)	24 (63.2)	16 (80.0)	<0.001 <sup>b</sup>	1-2, <i>p</i> < 0.001; 1-3, <i>p</i> < 0.001
	Normal	84 (67.2)	14 (36.8)	4 (20.0)		
N/L ratio (>3) (n=161)		(n=104)	(n=38)	(n=19)		
	High	28 (26.9)	15 (39.5)	13 (68.4)	0.002 <sup>b</sup>	1-3, <i>p</i> < 0.001; 2-3, <i>p</i> < 0.001; 1-2, <i>p</i> = 0.039
	Normal	76 (73.1)	23 (60.5)	6 (31.6)		
CRP (> 0.5 mg/dL) (n=170)		(n=113)	(n=38)	(n=19)		
	High	60 (53.1)	31 (81.6)	17 (89.5)	<0.001 <sup>b</sup>	1-2, <i>p</i> = 0.002; 1-3, <i>p</i> = 0.003
	Normal	53 (46.9)	7 (18.4)	2 (10.5)		
Ferritin (>291 ng/mL) (n=72)		(n=41)	(n=21)	(n=10)		
	High	19 (46.4)	10 (47.6)	7 (70.0)	0.393 <sup>b</sup>	NS
	Normal	22 (53.7)	11 (52.4)	3 (30.0)		
LDH (>234 IU/L) (n=62)		(n=31)	(n=18)	(n=13)		
	High	18 (58.2)	11 (61.1)	8 (61.5)	0.967 <sup>b</sup>	NS
	Normal	13 (41.9)	7 (38.9)	5 (38.5)		
D-dimer (>0.5 µg/mL) (n=77)		(n=37)	(n=25)	(n=15)		
	High	21 (56.8)	21 (84.0)	14 (93.3)	0.008 <sup>b</sup>	1-2, <i>p</i> = 0.024; 1-3, <i>p</i> = 0.011
	Normal	16 (43.2)	4 (16.0)	1 (6.7)		
Procalcitonin (> 0.5 ng/mL) (n=52)		(n=25)	(n=16)	(n=11)		
	High	15 (60.0)	9 (56.3)	5 (45.5)	0.720 <sup>b</sup>	NS
	Normal	10 (40.0)	7 (43.8)	6 (54.5)		

ICU, intensive care unit; COPD, chronic obstructive pulmonary disease; N/L, neutrophil to lymphocyte ratio; NS, not statistically significant; CRP, C-reactive protein; LDH, lactate dehydrogenase.

<sup>a</sup>Oneway ANOVA test and post hoc Bonferroni test; <sup>b</sup>Pearson chi-square test.

CT images were completely normal in 5 patients in Group 1, and one patient in Group 2. The other 8 cases had other typical or atypical findings (e.g., tree-in-bud, isolated

pleural thickening, effusion, fibrotic tape) instead of GGO.

The most common infiltration pattern in all groups was GGOs with a lower lobe

dominance. There was no statistically significant difference between the groups in terms of the rate of GGOs (*p* = 0.246). The rate of crazy-paving and consolidation



**Table 2.** Relationship between lung involvement pattern, distribution, percentage of affected lung parenchyma with groups

		Groups			p	Post hoc test
		Outpatient (n=172)	Inpatient (n=39)	ICU (n=20)		
		n (%)	n (%)	n (%)		
Ground-glass opacity	None (n=14)	13 (7.6)	1 (2.6)	0 (0)	0.246 <sup>a</sup>	
	Yes (n=217)	159 (92.4)	38 (97.4)	20 (100)		
Shape (n=217)	n	159	38	20	0.034 <sup>b</sup>	
	Round	61 (38.4)	6 (15.8)	8 (40.0)		
	Patchy	62 (39)	15 (39.5)	9 (45.0)		
	Mixed	33 (20.8)	17 (44.7)	3 (15.0)		
	Halo	3 (1.9)	0 (0)	0 (0)		
Diameter (n=217)	n	159	38	20	<0.001 <sup>c</sup>	1-2, p = 0.002; 1-3, p < 0.001
	Median (Q1–Q3)	2 (2–4)	5 (3–10)	5 (3–10)		
Right lower lobe (n=217)		118 (74.2)	35 (92.1)	14 (70.0)	0.046 <sup>a</sup>	
Left lower lobe (n=217)		107 (67.3)	32 (84.2)	15 (75.0)	0.109 <sup>a</sup>	
Right upper lobe (n=217)		70 (44.0)	29 (76.3)	14 (70.0)	<0.001 <sup>a</sup>	
Left upper lobe (n=217)		67 (42.1)	29 (76.3)	15 (75.0)	<0.001 <sup>a</sup>	
Right middle lobe (n=217)		35 (22.0)	22 (57.9)	10 (50.0)	<0.001 <sup>a</sup>	
Distribution	Peripheral (n=112)	83 (52.2)	17 (44.7)	7 (35.0)	0.368 <sup>b</sup>	
	Central (n=22)	18 (11.3)	2 (5.3)	2 (10.0)		
	Mixed (n=83)	55 (34.6)	18 (47.4)	10 (50.0)		
Consolidation	None (n=152)	123 (71.5)	22 (56.4)	7 (35.0)	0.002 <sup>a</sup>	1-3, p < 0.001
	Yes (n=79)	49 (28.5)	17 (43.6)	13 (65.0)		
Diameter (n=79)	n	49	17	13	0.190 <sup>c</sup>	NS
	Median (Q1–Q3)	3 (2.0–5.5)	3 (2.0–6.5)	6 (2.3–10)		
Right lower lobe (n=79)		25 (51.0)	13 (76.5)	12 (92.3)	0.010 <sup>a</sup>	
Left lower lobe (n=79)		23 (46.9)	9 (52.9)	10 (76.9)	0.156 <sup>a</sup>	
Right upper lobe (n =79)		14 (28.6)	8 (47.0)	7 (53.8)	0.148 <sup>a</sup>	
Left upper lobe (n =79)		13 (26.5)	5 (29.4)	4 (30.8)	0.943 <sup>a</sup>	
Right middle lobe (n =79)		7 (14.3)	6 (35.3)	3 (23.1)	0.172 <sup>a</sup>	
Distribution (n=79)	n	49	17	13	0.283 <sup>b</sup>	
	Peripheral (n=49)	30 (61.2)	12 (70.6)	7 (53.8)		
	Central (n=15)	10 (20.4)	4 (23.5)	1 (7.7)		
	Mixed (n=15)	9 (18.4)	1 (5.9)	5 (38.5)		
Crazy paving pattern (n=66)		37 (21.5)	20 (51.3)	9 (45)	<0.001 <sup>a</sup>	
Crazy paving pattern diameter	n	37	20	9	0.128 <sup>c</sup>	
	Median (Q1–Q3)	3 (3–5)	4 (3–5)	6 (3–10)		
Number of affected lobes	Median (Q1–Q3)	2 (1–4)	5 (3–5)	5 (3.3–5)	<0.001 <sup>c</sup>	1-2, p < 0.001; 1-3, p < 0.001
Total number of lesions	Median (Q1–Q3)	4 (1-10)	12 (4–20)	13.5 (5.3–20)	<0.001 <sup>c</sup>	1-2, p = 0.007; 1-3, p = 0.006
Percentage of affected lung parenchyma	(n=231)	175	39	20	<0.001 <sup>b</sup>	
	0	5 (2.9)	1 (2.6)	0 (0)		
	1	140 (81.4)	24 (61.5)	9 (45.0)		
	2	21 (12.2)	12 (30.8)	4 (20.0)		
	3	6 (3.5)	1 (2.6)	6 (30.0)		
	4	0 (0)	1 (2.6)	1 (5.0)		

ICU, intensive care unit; Q, quartile; NS, not statistically significant.

<sup>a</sup>Pearson chi-square test; <sup>b</sup>Fisher Freeman Halton Exact test; <sup>c</sup>Kruskal Wallis test and post hoc Dunn test.

**Table 3.** Relationship between typical and atypical CT findings with groups

		Groups			<i>P</i> <sup>a</sup>
		Outpatient (n=172)	Inpatient (n=39)	ICU (n=20)	
		n (%)	n (%)	n (%)	
CT features	Normal (n=6)	5 (2.9)	1 (2.6)	0 (0)	0.763
	Atypical (n=52)	45 (26.2)	8 (20.5)	5 (25.0)	
	Typical (n=173)	127 (73.8)	31 (79.5)	15 (75.0)	
Typical findings	Vascular enlargement (n=18)	11 (6.4)	7 (17.9)	0 (0)	0.021
	Fibrobant (n=70)	46 (26.7)	16 (41.0)	8 (40.0)	0.132
	Halo (n=41)	29 (16.9)	9 (23.1)	3 (15.0)	0.620
	Reverse halo (n=11)	7 (4.1)	4 (10.2)	0 (0)	0.151
Atypical findings	Tree-in-bud (n=6)	3 (1.7)	3 (7.7)	0 (0)	0.081
	Lobar consolidation (n=5)	0 (0)	2 (5.1)	3 (15.0)	<0.001
	Mediastinal lymphadenopathy (n=5)	0 (0)	0 (0)	5 (25.0)	<0.001
	Pleural effusion (n=15)	0 (0)	5 (12.8)	10 (50.0)	<0.001
	Pleural thickening (n=11)	4 (2.3)	2 (5.1)	5 (25.0)	0.001
	Air bronchogram (n=48)	27 (15.7)	13 (33.3)	8 (40.0)	0.004

ICU, intensive care unit; CT, computed tomography.

<sup>a</sup>Pearson chi-square test.

patterns was significantly higher in Group 3 than in Group 1 ( $p = 0.001$ ,  $p = 0.002$ , respectively). Right upper, left upper and right middle lobe GGO infiltrations were significantly higher in Group 3 ( $p = 0.001$ ). Rate of right upper, and right middle lobe involvements as consolidation pattern was significantly higher in Group 3 than in Group 1 ( $p = 0.148$ ,  $p = 0.172$ , respectively). There was a significant difference among the groups based on the number of affected lobes and the percentage of total lung parenchyma involvement ( $p = 0.001$ ) (Table 2). The average number of affected lobes was 2 in Group 1, while 4 lobes were affected in Groups 2 and 3 ( $p = 0.001$ ). The mean percentage of affected lung parenchyma percentage was 25% in Groups 1 and 2, and 50% in Group 3 ( $p = 0.001$ ). There was no statistically significant difference among groups based on presentation with typical or atypical CT imaging ( $p = 0.763$ ). However, in Group 3, the frequency of mediastinal LAP, pleural effusion, pleural thickening, and the presentation in the form of lobar consolidation was significantly higher than in the other groups ( $p = 0.001$ , for all). Fig. 3 shows three male patients in the same age range (80–90 years old) who were treated as an outpatient, inpatient, and in the ICU, with progressive worsening of CT imaging features. In contrast, Fig. 4 shows 3 male patients of the same age (40-year-old), who were treated as an outpatient, inpatient,

and in the ICU despite similar imaging features. CT imaging features of the patients are detailed in Table 3. Specificity, sensitivity, positive predictive value, and negative predictive value of CT imaging were 77.2%, 97.4%, 60%, and 98%, respectively. Interobserver reliability using kappa values was 0.923 (0.8–1, almost perfect agreement) ( $p = 0.001$ ).

## Discussion

Chest CT imaging findings for COVID-19 vary depending on the patients' immune response, underlying lung diseases, stage of disease at the time of scan, age, and presence of comorbidities. The typical radiological involvement for COVID-19 are GGOs, which are generally round lesions with a peripheral and subpleural distribution along with the bronchovascular bundle in lower lobes (8, 9). COVID-19 may also be visualized in the form of a crazy-paving pattern, where GGOs are accompanied by interlobular septal thickening or widespread consolidations are accompanied by bronchial wall thickening and air bronchograms (10–12). Occasionally, atypical findings such as pleural thickening-effusion, cavitation-pneumothorax, or mediastinal lymph node may occur alone or together with the typical imaging findings (9, 13). Numerous studies in the literature have shown GGOs and patchy consolidations to be the most frequently detected findings

on CT (14–16). In our study, GGOs were the most common CT finding in all groups, and its detection rate did not differ significantly based on the hospitalization pattern.

In their study, Li et al. (17) assessed the connection between imaging findings and clinical classification of COVID-19; their findings revealed that visual quantitative analysis of CT images showed high degree of consistency and can reflect COVID-19 clinical classification. The severe-critical type showed involvement of all 5 lobes, whereas common type usually showed involvement in the lower lobes (87%). In the severe type, the right middle and upper lobe involvement incidence were higher than the common type. Similarly, in our study, Group 3 patients, who had a severe clinical course, presented with more frequent involvement of both upper lobes and the right middle lobe, and had an average of 4 lobes affected. Colombi et al. (18) investigated the relation between well-aerated lung obtained on chest CT and COVID-19, and reported that patients that required ICU admission or expired had at least 4-lobe involvement similar to our study (18). In addition, they calculated the volume of well-aerated lung parenchyma on chest CT with visual or software quantification. Less than 73% of well-aerated lung parenchyma (more than 27% affected lung parenchyma) area was related to ICU admission or death. In our study, the mean percentage of affect-

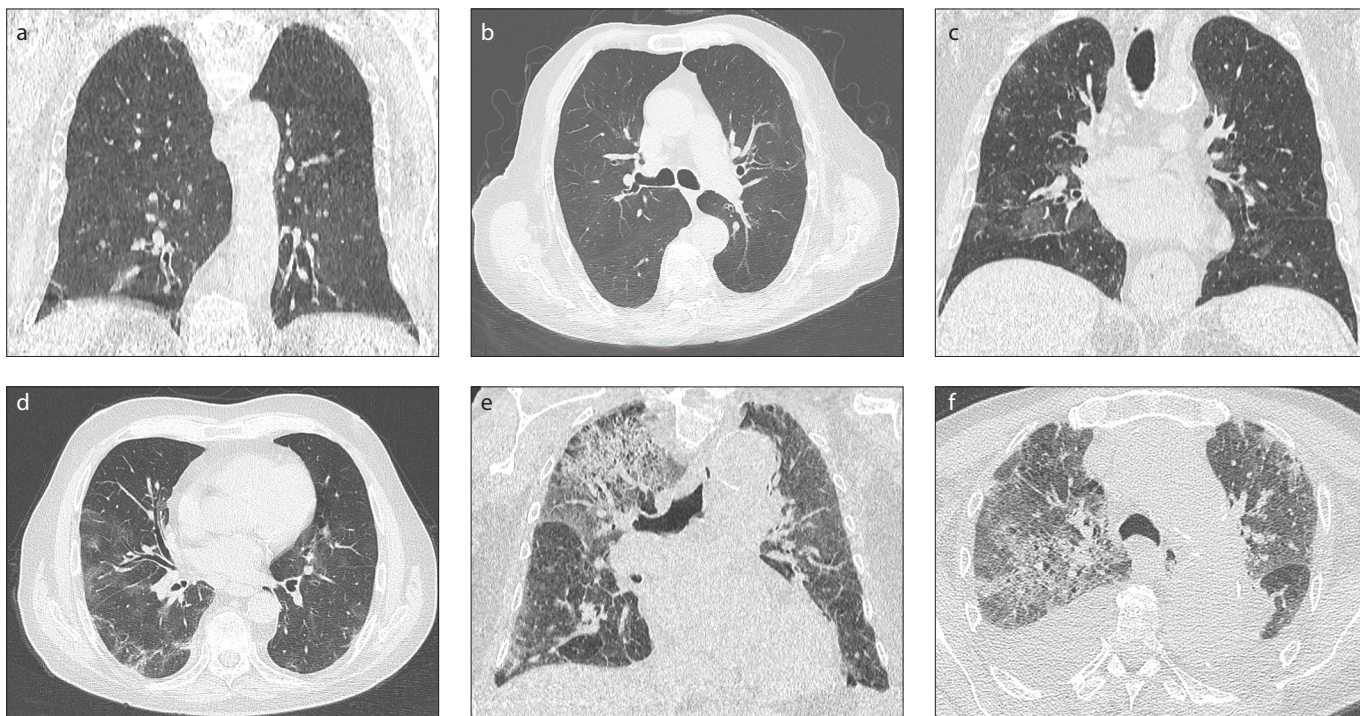


**Figure 3. a–f.** CT imaging features of 3 male cases in the same age range (80–90 years old) who were treated as an outpatient (a, b), inpatient (c, d), and in the intensive care unit (e, f). GGOs are limited to subpleural areas in the lower lobe bases in Group 1 case, GGOs are affecting all lobes showing peripheral dominance in Group 2 case. Group 3 case shows diffuse GGOs infiltration up to both upper lobe apicals dominated by crazy-paving pattern. Note that both lower lobes are infiltrated by consolidations accompanied by pleural effusion. As involvement in form of widespread crazy-paving pattern  $\pm$  consolidation, and/or affected lung parenchyma areas increase towards the upper lobes, a worse prognosis may be anticipated.

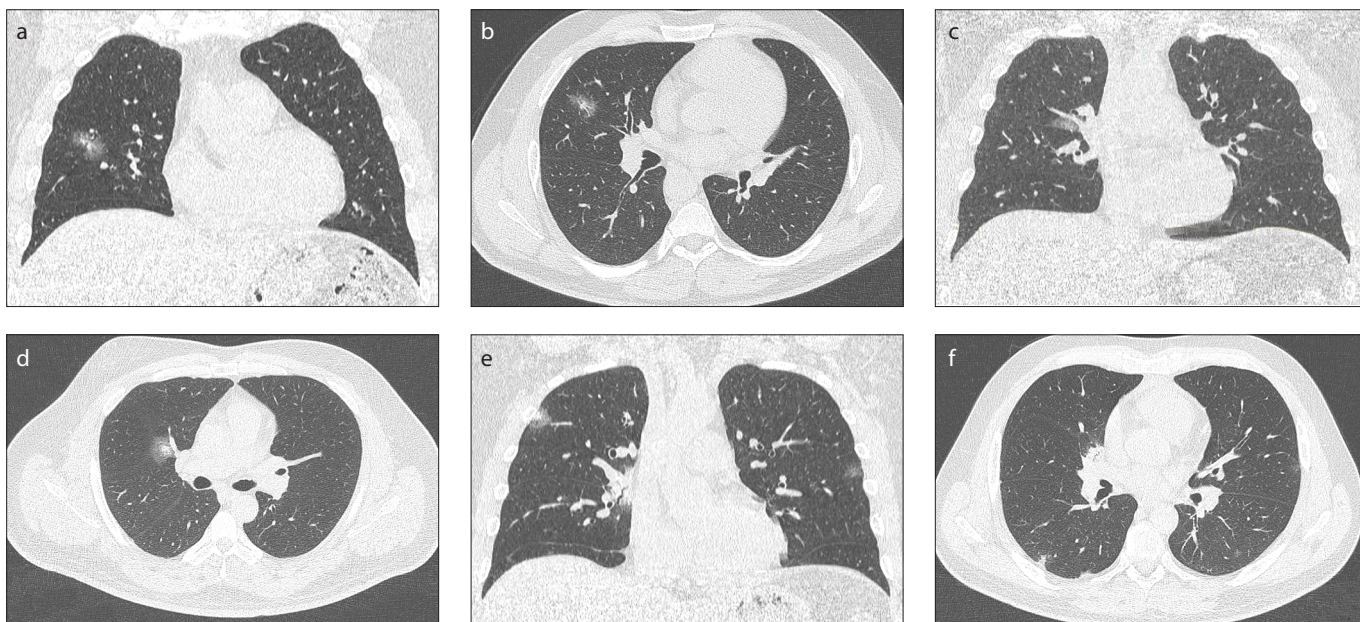


**Figure 4. a–f.** Coronal and axial CT images of 3 male patients of the same age (40-year-old), who were treated as outpatient (a, b), inpatient (c, d) and in the intensive care unit (e, f). They have similar diameters and infiltration patterns in the form of consolidation and ground-glass opacities in the right upper and middle lobe, distributed centrally and peripherally in the chest CT images. Estimating the prognosis with only CT imaging features may be misleading.

ed lung parenchyma in Group 3 was 50%, which is higher than their study. Tabatabaei et al. (19) examined the relationship of involvement pattern and distribution with prognosis; Group 3 and nonsurvivors had

more frequent consolidation, crazy-paving pattern, and central lung involvement compared to hospitalized patient with routine admission process, similar to our study. It is considered that consolidation pattern,

central involvement, and pleural effusion in the initial chest CT, increase in the number of affected lobes and extent of affected parenchyma are more common in critically ill patients.



Song et al. (20) showed that CT findings differ markedly by age groups and in particular the consolidative infiltration pattern is associated with progressive disease. In our study, the mean age of Group 2/3 patients was higher than that of Group 1 patients, and crazy-paving and consolidation pattern were significantly more prevalent in Groups 2 and 3. Studies in the literature reported that approximately 7% of cases show atypical imaging findings (8, 21), and atypical CT findings are mostly seen in elderly patients (9, 21). In our study group, atypical CT findings were more prevalent compared to the literature, but there was no significant difference between the groups. However, in ICU patients, mediastinal LAP, pleural effusion, thickening rates, and the presentation in the form of lobar consolidation were significantly higher compared with other groups.

Chung et al. (8) showed that in 38% of cases, 5 lobes were affected and the most commonly affected lobe was the lower right lobe (76%) and the least affected was the right middle lobe. In our study, a similar distribution was obtained, and the right and left lower lobes were most frequently involved in all groups. Both upper (74%, 84%) and right middle lobe (56%, 54%) involvements were significantly higher in Group 2 and Group 3 compared with Group 1. This suggests that the involvement of these localizations at initial scanning may be related to subsequent hospitalization. As the number of affected lobes and lung parenchyma area increases, these cases showed a more severe clinical course and respiratory distress (Fig. 3) (22). In our study group, the need for hospitalization or respiratory support increased as the number of lobes involved with the affected lung parenchyma area increased.

Apart from all these, we see that the clinical course is different in some cases presenting with similar infiltration patterns of the same age and gender (Fig. 4). At this point, comorbid diseases and the immune status of the patient are predictive in terms of prognosis. In these patients, disease-specific laboratory parameters are often correlated with the severity of the disease, thus guiding clinicians in the follow-up of patients (23).

This study has some limitations. The major limitation is that there is no standard timing for CT screening, since each patient may be symptomatic at a different stage of the disease or the stage of the disease at the time of presentation may differ from person to person, and CT imaging findings may differ considering the stage of the disease. In addition, the retrospective and single-center design is another limitation.

In conclusion, the findings of the current study indicate that admission to ICU increases as number of affected lung lobes and percentage of affected lung parenchyma increase at initial chest CT examination. However, it should be kept in mind that CT findings are not the only determinant factor for prognosis and these findings should be evaluated together with patients' age, comorbidities, and laboratory parameters.

#### Conflict of interest disclosure

The authors declared no conflicts of interest.

#### References

1. Singhal T. A review of coronavirus disease-2019 (COVID-19). *Indian J Pediatr* 2020; 87:281–286. [\[Crossref\]](#)
2. Fang Y, Zhang H, Xie J, et al. Sensitivity of chest CT for COVID-19: comparison to RT-PCR. *Radiology* 2020; 296:E115–117. [\[Crossref\]](#)
3. Long C, Xu H, Shen Q, et al. Diagnosis of the coronavirus disease (COVID-19): rRT-PCR or CT? *Eur J Radiol* 2020; 126:108961. [\[Crossref\]](#)
4. Wang YXJ, Liu W-H, Yang M, Chen W. The role of CT for Covid-19 patient's management remains poorly defined. *Ann Transl Med* 2020; 8:145. [\[Crossref\]](#)
5. Jin YH, Cai L, Cheng ZS, et al. A rapid advice guideline for the diagnosis and treatment of 2019 novel coronavirus (2019-nCoV) infected pneumonia (standard version). *Mil Med Res* 2020; 7:4. [\[Crossref\]](#)
6. Zhang W, Zhao Y, Zhang F, et al. The use of anti-inflammatory drugs in the treatment of people with severe coronavirus disease 2019 (COVID-19): The experience of clinical immunologists from China. *Clin Immunol* 2020; 214:108393. [\[Crossref\]](#)
7. Bhatraju PK, Ghassemieh BJ, Nichols M, et al. COVID-19 in critically ill patients in the Seattle region — Case series. *N Engl J Med* 2020; 382:2012–2022. [\[Crossref\]](#)
8. Bernheim A, Mei X, Huang M, et al. Chest CT Findings in coronavirus disease-19 (COVID-19): relationship to duration of infection. *Radiology* 2020; 295:200463. [\[Crossref\]](#)
9. Chung M, Bernheim A, Mei X, et al. CT imaging features of 2019 novel coronavirus (2019-nCoV). *Radiology* 2020; 295:202–207. [\[Crossref\]](#)

10. Guneyli S, Atceken Z, Dogan H, Altinmakas E, Atasoy KC. Radiological approach to COVID-19 pneumonia with an emphasis on chest CT. *Diagn Interv Radiol* 2020; 26:323–332. [\[Crossref\]](#)
11. Ye Z, Zhang Y, Wang Y, Huang Z, Song B. Chest CT manifestations of new coronavirus disease 2019 (COVID-19): a pictorial review. *Eur Radiol* 2020. Published online 19 Mar 2020. [\[Crossref\]](#)
12. Sun Z, Zhang N, Li Y, Xu X. A systematic review of chest imaging findings in COVID-19. *Quant Imaging Med Surg* 2020; 10:1058–1079. [\[Crossref\]](#)
13. Liew JRP, Lim YRD, Liew JYC, Poh CCA. Clinics in diagnostic imaging: COVID-19 atypical pneumonia. *Singapore Med J* 2020; 61:363–369.
14. Chen N, Zhou M, Dong X, et al. Epidemiological and clinical characteristics of 99 cases of 2019 novel coronavirus pneumonia in Wuhan, China: a descriptive study. *Lancet* 2020; 395:507–513. [\[Crossref\]](#)
15. Pan Y, Guan H, Zhou S, et al. Initial CT findings and temporal changes in patients with the novel coronavirus pneumonia (2019-nCoV): a study of 63 patients in Wuhan, China. *Eur Radiol* 2020; 30:3306–3309. [\[Crossref\]](#)
16. Wang D, Hu B, Hu C, et al. Clinical characteristics of 138 hospitalized patients with 2019 novel coronavirus-infected pneumonia in Wuhan, China. *JAMA* 2020; 323:1061. [\[Crossref\]](#)
17. Li K, Fang Y, Li W, et al. CT image visual quantitative evaluation and clinical classification of coronavirus disease (COVID-19). *Eur Radiol* 2020; 30:4407–4416. [\[Crossref\]](#)
18. Colombi D, Bodini FC, Petrini M, et al. Well-aerated lung on admitting chest CT to predict adverse outcome in COVID-19 pneumonia. *Radiology* 2020; 296:E86–96. [\[Crossref\]](#)
19. Tabatabaei SMH, Talari H, Moghaddas F, Rajebi H. Computed tomographic features and short-term prognosis of coronavirus disease 2019 (COVID-19) pneumonia: a single-center study from Kashan, Iran. *Radiol Cardiothorac Imaging* 2020; 2:e200130. [\[Crossref\]](#)
20. Song F, Shi N, Shan F, et al. Emerging 2019 novel coronavirus (2019-nCoV) pneumonia. *Radiology* 2020; 295:210–217. [\[Crossref\]](#)
21. Salehi S, Abedi A, Balakrishnan S, Gholamrezanezhad A. Coronavirus disease 2019 (COVID-19): a systematic review of imaging findings in 919 patients. *Am J Roentgenol* 2020; 215:87–93. [\[Crossref\]](#)
22. Lomoro P, Verde F, Zerboni F, et al. COVID-19 pneumonia manifestations at the admission on chest ultrasound, radiographs, and CT: single-center study and comprehensive radiologic literature review. *Eur J Radiol Open* 2020; 7:100231. [\[Crossref\]](#)
23. Guan WJ, Liang WH, Zhao Y, et al. Comorbidity and its impact on 1590 patients with COVID-19 in China: a nationwide analysis. *Eur Respir J* 2020; 55:2000547. [\[Crossref\]](#)